Subspace representations in *ab initio* methods for strongly correlated systems

David D. O'Regan,[1,*] Mike C. Payne,[1] and Arash A. Mostofi[2]
[1]*Cavendish Laboratory, University of Cambridge, J. J. Thomson Avenue, Cambridge CB3 0HE, United Kingdom*
[2]*The Thomas Young Centre, Imperial College London, London SW7 2AZ, United Kingdom*
(Received 9 February 2011; revised manuscript received 12 April 2011; published 27 June 2011)

We present a generalized definition of subspace occupancy matrices in *ab initio* methods for strongly correlated materials, such as DFT+U (density functional theory + Hubbard U) and DFT+DMFT (dynamical mean-field theory), which is appropriate to the case of nonorthogonal projector functions. By enforcing the tensorial consistency of all matrix operations, we are led to a subspace-projection operator for which the occupancy matrix is tensorial and accumulates only contributions which are local to the correlated subspace at hand. For DFT+U, in particular, the resulting contributions to the potential and ionic forces are automatically Hermitian, without resort to symmetrization, and localized to their corresponding correlated subspace. The tensorial invariance of the occupancies, energies, and ionic forces is preserved. We illustrate the effect of this formalism in a DFT+U study using self-consistently determined projectors.

DOI: 10.1103/PhysRevB.83.245124 PACS number(s): 71.15.Mb, 31.15.E−, 71.15.Ap

I. INTRODUCTION

The routine *ab initio* study of strongly correlated systems, that is those for which the accurate description of the physics is beyond the capacity of mean-field methods such as Kohn–Sham density functional theory[1] (DFT) within local or semilocal approximations to the exchange-correlation (XC) functional, remains a challenge for electronic structure calculations.

A number of sophisticated methods to correct the description of strong correlation effects within DFT have been developed which provide a good compromise between accuracy and computational expense. Successful examples include calculations using self-interaction corrected XC functionals,[2] exact exchange in DFT,[3] and the GW Approximation,[4] among others. Here we focus on methods, notably DFT+U (DFT+Hubbard U)[5] and DFT+DMFT (dynamical mean-field theory)[6] for static and dynamical spatially localized correlation effects, respectively, which share a common history and conceptual motivation based on models for Coulomb interactions such as the renowned Hubbard model.[7]

In such methods, the electronic system is subdivided into a set of spatially localized correlated subspaces, the description of the interactions in which is deemed to be beyond the capacity of the approximate XC functional, and the remainder which acts as a bath for particle exchange and for which, due to its having a large kinetic energy relative to Coulomb repulsion, the approximate XC functional performs adequately. In this manner, a model interaction may be used to augment and improve the description of the screened Coulomb interactions between densities in the correlated subspaces while retaining the computationally inexpensive XC approximation for the remainder of the system. Generally for these methods, the occupancy matrix of each correlated subspace is the object which provides the necessary information on the electronic density to the model describing intra-subspace interactions. Defining the occupancy matrix of a correlated subspace using a set of orthonormal projectors is quite straightforward, yet the question of how to properly extend the formalism to allow for the possibility of nonorthogonal spanning functions is one under active debate[8,9] and one of immediate practical consequence.

It is frequently useful to permit the nonorthogonality of the basis functions for the Kohn–Sham[1] states in *ab initio* methods which make use of sophisticated spatially localized orbitals for such functions, particularly in linear-scaling DFT methods.[8,10–12] Additionally, either for reasons of computational convenience, as in Refs. 8,13,14, or for the purposes of achieving self-consistency over the correlated subspaces, as in Ref. 15, it is common to use a subset of these nonorthogonal basis functions as projectors for the correlated subspaces, the subset termed *Hubbard projectors*. We demonstrate here, however, that it may be hazardous to overidentify the Hubbard projectors with the basis set from which they are drawn.

In this paper, we offer a revised definition of the subspace occupancy matrix for *ab initio* methods which use nonorthogonal projectors to define the strongly correlated subspaces. We show that, by enforcing the tensorial consistency of all matrix operations, we are led immediately to a simple definition of the projection operator for each subspace which is fully localized to that subspace. In contrast to previously proposed formalisms of Ref. 8 and references therein, this gives rise to Hermitian corrections to the potential and ionic forces, without any *post hoc* symmetrization, which are also localized to the spaces in which the correlation correction is required. The resulting occupancy matrix reproduces the electron number of the subspaces and is tensorial. Thus, for example, its trace is invariant under both unitary rotations and the generalized Löwdin transformations[16] of Ref. 9.

To illustrate the performance of the proposed formalism, we applied it to the DFT+U method in a study of two strongly correlated systems, namely bulk nickel oxide and the gas-phase copper phthalocyanine dimer, with comparison to the most comprehensive alternative formalism available at the time of writing, the "dual representation" of Ref. 8. A set of nonorthogonal generalized Wannier functions (NGWFs),[10] optimized using the projector self-consistent DFT+U method described in Ref. 15, was used to carry out our computational study with a minimum of user intervention in the construction of the nonorthogonal Hubbard projectors.

II. NONORTHOGONAL REPRESENTATIONS OF THE OCCUPANCY MATRIX

Generally, to extract low-energy Hubbard-type models from *ab initio* DFT simulations, we require the projection of the single-particle density matrix

$$\hat{\rho}^{(\sigma)} = \sum_{i\mathbf{k}} \left|\psi_{i\mathbf{k}}^{(\sigma)}\right\rangle f_{i\mathbf{k}}^{(\sigma)} \left\langle\psi_{i\mathbf{k}}^{(\sigma)}\right|, \tag{1}$$

where $\psi_{i\mathbf{k}}^{(\sigma)}$ is a Kohn–Sham eigenstate for spin channel σ with band index i, crystal momentum $\mathbf{k}$, and occupancy $f_{i\mathbf{k}}^{(\sigma)}$, onto a set of spatially localized subspaces. These subspaces $\mathcal{C}^{(I)}$, where I is the site index, encompass that part of the Hilbert space of the Kohn–Sham orbitals which is deemed to be responsible for strong localized Coulomb interactions beyond the scope of the approximate XC functional.

The occupancy of subspace $\mathcal{C}^{(I)}$, which is delineated by a set of $M^{(I)}$ potentially nonorthogonal spanning projectors $|\varphi_m^{(I)}\rangle$, $m \in \{1, \ldots, M^{(I)}\}$, dubbed *Hubbard projectors*, which are associated with subspace I, is generally given by the subspace-projected density matrix

$$\hat{n}^{(I)(\sigma)} = \hat{P}^{(I)\dagger} \hat{\rho}^{(\sigma)} \hat{P}^{(I)}. \tag{2}$$

The Hubbard projection operator $\hat{P}^{(I)}$, the resolution of the identity for the space $\mathcal{C}^{(I)}$, is defined in terms of the Hubbard projectors, but the exact manner in which this definition should be made has been the subject of some discussion, as we describe in the following.

Some important conditions should be satisfied by a sound definition of the occupancy matrix of each correlated site, namely, all operations such as matrix products and traces should be tensorially consistent so that the total energy, potential, and forces are tensorial invariants (unaltered by arbitrary transformations of the basis on which the projectors for that site are defined); any potential depending on that occupancy matrix should be Hermitian and its action should be strictly localized to the correlated subspace while depending only on occupancies which are themselves localized to that subspace; the trace of the occupancy matrix should exactly reproduce the occupancy of the correlated manifold on that site; and if the site is extended to encompass the entire system then the total electron number should be obtained.

A. The "full" and "on-site" representations

We generally assume that a set of complex, mutually nonorthogonal Hubbard projectors are used for each individual site and that the correlated subspaces possibly overlap (we do not consider transformations among the projectors of different correlated sites). Dual vectors of the Hubbard projectors must be defined with respect to some Hilbert superspace of the correlated manifold, $\mathcal{H}^{(I)} \supseteq \mathcal{C}^{(I)}$, some possibilities for which are the subspace itself (i.e., $\mathcal{H}^{(I)} = \mathcal{C}^{(I)}$), the union of all correlated subspaces (i.e., $\mathcal{H}^{(I)} = \bigcup_I \mathcal{C}^{(I)}$), and the space $\mathcal{S}$ spanned by all basis functions in the simulation cell (i.e., $\mathcal{H}^{(I)} = \mathcal{S}$). The Hubbard projector duals are then generally given by

$$|\varphi^{(I)m}\rangle = \sum_{\alpha \in \mathcal{H}^{(I)}} \left|\varphi_\alpha^{(I)}\right\rangle S^{(I)\alpha m}, \tag{3}$$

where $S^{(I)\bullet\bullet}$ is the contravariant metric tensor for the set of functions spanning $\mathcal{H}^{(I)}$ (the inverse of their overlap matrix). Physically meaningful inner products, e.g., tensorial invariants such as occupancies, energies or forces, are computed between functions and elements of their set of dual functions only (in the orthonormal case there is no practical distinction between functions and their duals). For a more detailed exposition of tensor calculus applied to problems in electronic structure theory, we refer the reader to Ref. 17.

It is immediately clear that the simplest definition of the occupancy matrix for a given site, that is, the projection $\hat{P}^{(I)} = \sum_{m \in \mathcal{C}^{(I)}} |\varphi_m^{(I)}\rangle\langle\varphi_m^{(I)}|$ of the valence manifold over the site's Hubbard projectors,

$$n_{mm'}^{(I)(\sigma)} = \left\langle\varphi_m^{(I)}\right|\hat{\rho}^{(\sigma)}\left|\varphi_{m'}^{(I)}\right\rangle, \tag{4}$$

is invalid for nonorthogonal projectors. This widely used definition of the occupancy matrix, which is entirely appropriate in the orthonormal case, such as calculations described in Ref. 18 and numerous citations therein, simply neglects all nonorthogonality; the trace or powers of such a fully covariant tensor are not physically meaningful in the nonorthogonal case.

A total site occupancy defined as a trace operation on this matrix, as in

$$N^{(I)(\sigma)} = \sum_m n_{mm}^{(I)(\sigma)}, \tag{5}$$

implies that such an occupancy is not, in general, a tensorial invariant since it is formed by a tensorially invalid summation over two covariant indices–as opposed to a meaningful contraction of indices of opposite tensor character. Occupancies, just like total energies, should be tensorial invariants, scalars which are unchanged by transformations of the basis on which the projector functions are defined.

Progress was made in the definition of the occupancies of correlated subspaces via nonorthogonal projectors when it was noted[14] that tensorially contravariant projector duals should be involved, a concept known in other contexts for some time.[19] A definition of the occupancy matrix fully in terms of Hubbard projector duals was described in Ref. 14, for example, where the projection operator defined as $\hat{P}^{(I)} = \sum_{m \in \mathcal{C}^{(I)}} |\varphi^{(I)m}\rangle\langle\varphi^{(I)m}|$, provides an occupancy matrix

$$\begin{aligned} n^{(I)(\sigma)mm'} &= \langle\varphi^{(I)m}|\hat{\rho}^{(\sigma)}|\varphi^{(I)m'}\rangle \\ &= S^{(I)m\alpha}\left\langle\varphi_\alpha^{(I)}\right|\hat{\rho}^{(\sigma)}\left|\varphi_\beta^{(I)}\right\rangle S^{(I)\beta m'}. \end{aligned} \tag{6}$$

The indices α and β run over the spanning vectors of the contravariant metric (i.e., the inverse overlap matrix) $S^{(I)\bullet\bullet}$, on a superspace $\mathcal{H}^{(I)}$ of the correlated manifold $\mathcal{C}^{(I)}$. Here and hereafter, we make use of the summation convention,[20] whereby repeated indices within the same expression are summed over unless in parentheses.

Unfortunately, the matrix trace and powers of Eq. (6) are not tensorially valid, as can be seen by taking the example of the square of this contravariant occupancy matrix, which is of interest for density-density self-interaction corrections to

approximate XC functionals. The resulting expression for the squared occupancy matrix,

$$n^{2(I)(\sigma)mm'} = \sum_{m'' \in \mathcal{C}^{(I)}} n^{(I)(\sigma)mm''} n^{(I)(\sigma)m''m'}, \tag{7}$$

implies that the operator

$$\hat{P}^{(I)} = \sum_{m'' \in \mathcal{C}^{(I)}} |\varphi^{(I)m''}\rangle\langle\varphi^{(I)m''}| \tag{8}$$

forms a tensorially traceable identity on $\mathcal{C}^{(I)}$. It does not in the case of nonorthogonal projectors, however, since an identity operator may be formed only via the outer product between a projector and a projector dual, and not a dual vector and its own complex conjugate, including the case where the correlated subspace is extended to the Hilbert space of the entire system ($\mathcal{C}^{(I)} = \mathcal{S}$).

The shortcomings in the two definitions of the occupancy matrix described above have been previously described in detail by Han *et al*. in Ref. 8 and are dubbed, respectively, the "full" [Eq. (4)] and "on-site" [Eq. (6)] representations in the nomenclature described therein. These authors concentrated on the special case where the dual-generating superspace $\mathcal{H}^{(I)}$ is the space spanned by all basis functions $\{|\phi_\alpha\rangle\}$ in the simulation cell, so that $\mathcal{H}^{(I)} = \mathcal{S}$, in which case $S_{\alpha\beta} = \langle\phi_\alpha|\phi_\beta\rangle$ and the Hubbard projectors form a subset of the basis set. Thus, the same contravariant metric for all basis functions in the simulation cell is used to generate the dual functions on each correlated site, and in this case the full and on-site occupancy matrices simplify, respectively, to

$$n^{(I)(\sigma)}_{mm'} = \sum_{\alpha,\beta \in \mathcal{S}} S_{m \in \mathcal{C}^{(I)}\alpha} K^{(\sigma)\alpha\beta} S_{\beta m' \in \mathcal{C}^{(I)}} \quad \text{and} \tag{9}$$

$$n^{(I)(\sigma)mm'} = K^{(\sigma)m \in \mathcal{C}^{(I)} m' \in \mathcal{C}^{(I)}}. \tag{10}$$

Here, $K^{(\sigma)\alpha\beta} = \langle\phi^\alpha|\hat{\rho}^{(\sigma)}|\phi^\beta\rangle$ is the representation of the density matrix in terms of basis-set duals, known as the density kernel. The notation $S_{m \in \mathcal{C}^{(I)}\alpha}$ reminds us that m and α run over the spanning vectors of two different spaces, $\mathcal{C}^{(I)}$ and $\mathcal{H}^{(I)} = \mathcal{S}$, respectively, so that the block of $S_{\bullet\bullet}$ in question is generally not square.

B. The "dual" representation

Han *et al*.,[8] whose invaluable contribution on this subject addressed many of the salient issues, pointed out that the total number of electrons is not recovered by the trace of the occupancy matrix if the site is extended to include the entire simulation cell using the full and on-site representations. They proposed an alternative "dual" representation which solves this particular problem and is generated by the projector

$$\hat{P}^{(I)} = \frac{1}{2} \sum_{m \in \mathcal{C}^{(I)}} \left(|\varphi^{(I)m}\rangle\langle\varphi^{(I)}_m| + |\varphi^{(I)}_m\rangle\langle\varphi^{(I)m}| \right) \tag{11}$$

and the corresponding occupancy matrix

$$\begin{aligned} &\frac{1}{2}\left(\langle\varphi^{(I)m}|\hat{\rho}^{(\sigma)}|\varphi^{(I)}_{m'}\rangle + \langle\varphi^{(I)}_m|\hat{\rho}^{(\sigma)}|\varphi^{(I)m'}\rangle \right) \\ = &\frac{1}{2} \sum_{\alpha \in \mathcal{S}} \left(K^{(\sigma)m \in \mathcal{C}^{(I)}\alpha} S_{\alpha m' \in \mathcal{C}^{(I)}} + S_{m \in \mathcal{C}^{(I)}\alpha} K^{(\sigma)\alpha m' \in \mathcal{C}^{(I)}} \right). \end{aligned} \tag{12}$$

In the dual representation, the contravariant metric on the basis set is used to form the Hubbard projector duals (which are therefore delocalized across the entire simulation cell, in general, since the inverse overlap matrix is dense even when the overlap matrix itself is sparse) via $|\varphi^{(I)m}\rangle = \sum_{\alpha \in \mathcal{S}} |\varphi^{(I)}_\alpha\rangle S^{\alpha m}$. Symmetrization is then carried out to both provide a symmetric occupancy matrix and to recover a Hermitian potential.

The dual representation shares with the full representation the attribute of Hermiticity and, furthermore, it has a tensorially and physically meaningful trace. As such, to our knowledge, it provides the most favorable occupancy definition hitherto available. However, this occupancy matrix is tensorially ambiguous, consisting of the sum of tensors of differing index character.

One cannot generally symmetrize or antisymmetrize a tensor over indices of mixed covariant and contravariant character in this way and obtain a matrix which transforms as a tensor (one which may be used to generate tensorially invariant occupancies, local moments, or energies). Thus, while providing a significant improvement over previously suggested definitions of the occupancy matrix due to its tensorially invariant trace, the dual representation suffers similar problems with matrix powers as other representations: If we attempt to compute the square of this matrix we obtain tensorially inconsistent, and thus physically meaningless, terms in the product, of the form $n^{m}{}_{m''} n^{m'}_{m''}$ and $n_{m}{}^{m''} n^{m''}_{m'}$.

C. Requirement for a subspace-localized Hermitian projection operator

Let us step back for a moment and consider why any projection operator of the form

$$\hat{P}^{(I)} = \sum_{\substack{m \in \mathcal{C}^{(I)} \\ \alpha \in \mathcal{H}^{(I)} \neq \mathcal{C}^{(I)}}} |\varphi^{(I)}_\alpha\rangle S^{\alpha m} \langle\varphi^{(I)}_m| \tag{13}$$

requires symmetrization to the dual form in order to provide a Hermitian potential operator.

An arbitrary potential operator $\hat{V}$, operating on the subspace $\mathcal{C}^{(I)}$, which could represent the screened Coulomb interaction, for example, has matrix elements in the frame of Hubbard projectors given by

$$V^{(I)mm'}_m = \sum_{\alpha \in \mathcal{H}^{(I)}} \langle\varphi^{(I)}_m|\hat{V}|\varphi^{(I)}_\alpha\rangle S^{\alpha m'}. \tag{14}$$

The potential operator is easily shown to be non-Hermitian in the case where $m, m' \in \mathcal{C}^{(I)} \subset \mathcal{H}^{(I)} \subseteq \mathcal{S}$, and $\mathcal{C}^{(I)} \neq \mathcal{H}^{(I)}$ strictly holds, since

$$\begin{aligned} \hat{V}^{(I)} &= \hat{P}^{(I)\dagger} \hat{V} \hat{P}^{(I)} = |\varphi^{(I)}_m\rangle V^{(I)mm'} \langle\varphi^{(I)}_{m'}| \\ &= \sum_{\alpha,\beta \in \mathcal{H}^{(I)}} |\varphi^{(I)}_m\rangle S^{(I)m\alpha} V^{(I)}_{\alpha\beta} S^{(I)\beta m'} \langle\varphi^{(I)}_{m'}| \\ &\neq \sum_{\alpha,\beta \in \mathcal{H}^{(I)}} |\varphi^{(I)}_\alpha\rangle S^{(I)\alpha m} V^{(I)}_{mm'} S^{(I)m'\beta} \langle\varphi^{(I)}_\beta| \\ &= |\varphi^{(I)m}\rangle V^{(I)}_{mm'} \langle\varphi^{(I)m'}| = \hat{P}^{(I)} \hat{V} \hat{P}^{(I)\dagger} = \hat{V}^{(I)\dagger}. \end{aligned} \tag{15}$$

The reason for this non-Hermiticity is that the indices α, β do not generally run over functions spanning just the correlated space $\mathcal{C}^{(I)}$, but rather over those that span a superspace $\mathcal{H}^{(I)}$,

e.g., typically over the basis functions in the simulation cell, $\mathcal{H}^{(I)} = \mathcal{S}$. This observation is quite general: The dual projectors must be constructed using the metric on *precisely* the space spanned by the projectors themselves in order to build a Hermitian projection operator and hence a Hermitian potential. This cannot be circumvented in a tensorially consistent way by symmetrizing operators since tensors can be symmetrized over pairs of indices only if they are either both of covariant character or both of contravariant character.

D. The "tensorial" representation

Based on the above, we deduce that to build a tensorially consistent occupancy matrix which generates a Hermitian potential, the projection operator for a given subspace $\mathcal{C}^{(I)}$ must necessarily be constructed using exact dual Hubbard projectors with respect to that subspace only. Thus, with the covariant overlap matrix of Hubbard projectors defined by

$$O^{(I)}_{mm'} = \langle \varphi^{(I)}_m | \varphi^{(I)}_{m'} \rangle, \tag{16}$$

that is, an *individual* $M^{(I)} \times M^{(I)}$ covariant metric tensor for each correlated site I, the proper dual vectors $|\varphi^{(I)m}\rangle$ are constructed using the corresponding contravariant metric $O^{(I)m'm}$, as per

$$|\varphi^{(I)m}\rangle = \sum_{m' \in \mathcal{C}^{(I)}} |\varphi^{(I)}_{m'}\rangle O^{(I)m'm}. \tag{17}$$

Here, we emphasize that the contravariant metric is obtained via a separate $M^{(I)} \times M^{(I)}$ inverse operation for each site, so that

$$O^{(I)m'm''} O^{(I)}_{m''m} = \delta^{m'}_{\ m}. \tag{18}$$

In the special case where the Hubbard projectors are drawn from the set of functions used to represent the Kohn–Sham wave functions, the overlap matrix of duals $O^{(I)\bullet\bullet}$ for each site cannot generally be extracted immediately from the metric $S^{\bullet\bullet}$ on $\mathcal{S}$. However, in this particular case, the $O^{(I)}_{\bullet\bullet}$ matrix for each site is merely a sub-block of the basis-function overlap $S_{\bullet\bullet}$ and, from this, the contravariant $O^{(I)\bullet\bullet}$ for each site can be computed by a separate inverse operation for each site which is typically fast, due to the small matrix dimension.

Employing this definition of the metric tensor on each subspace, the projector duals remain manifestly as localized to the correlated subspace as the projectors themselves; they pick up only subspace-localized contributions to the occupancy and can apply only subspace-localized corrective potentials, as we would expect for local self-interaction corrections such as DFT+U or its extensions. The Hubbard projection operator, in what we will denote the "tensorial" representation,

$$\hat{P}^{(I)} = \sum_{m,m' \in \mathcal{C}^{(I)}} |\varphi^{(I)}_{m'}\rangle O^{m'm} \langle \varphi^{(I)}_m|, \tag{19}$$

is Hermitian and thus gives rise to a Hermitian potential, without resort to symmetrization, since $O^{(I)\bullet\bullet}$ is a square overlap matrix:

$$\begin{aligned} \hat{V}^{(I)} &= \hat{P}^{(I)\dagger} \hat{V} \hat{P}^{(I)} = |\varphi^{(I)}_m\rangle V^{(I)mm'} \langle \varphi^{(I)}_{m'}| \\ &= |\varphi^{(I)}_m\rangle O^{(I)mm'} V^{(I)}_{m'm''} O^{(I)m''m'''} \langle \varphi^{(I)}_{m'''}| \\ &= |\varphi^{(I)m}\rangle V^{(I)}_{mm'} \langle \varphi^{(I)m'}| = \hat{P}^{(I)} \hat{V} \hat{P}^{(I)\dagger} = \hat{V}^{(I)\dagger}. \end{aligned} \tag{20}$$

The occupancy matrix is most easily expressed in its singly covariant and singly contravariant form, though other forms are readily obtainable from the metric tensor, so manipulations of the following form can be made:

$$n_{\bullet}^{\ \bullet} = O_{\bullet\bullet} n^{\bullet\bullet} = n_{\bullet\bullet} O^{\bullet\bullet} = O_{\bullet\bullet} n^{\bullet}_{\ \bullet} O^{\bullet\bullet}. \tag{21}$$

The contravariant-covariant or covariant-contravariant forms of the tensorial occupancy matrix, the latter given by (the second line applies to the special case where Hubbard projectors are drawn from the basis set)

$$\begin{aligned} n^{(I)(\sigma)m'}_{\quad m} &= \langle \varphi^{(I)}_m | \hat{\rho}^{(\sigma)} | \varphi^{(I)}_{m''} \rangle O^{(I)m''m'} \\ &= \sum_{\alpha,\beta \in \mathcal{S}} S_{m\alpha} K^{\alpha\beta} S_{\beta m''} O^{(I)m''m'}, \end{aligned} \tag{22}$$

possess a common tensorially invariant trace (a proper contraction over one covariant and one contravariant index) which recovers the exact number of electrons in the correlated subspace by construction (the so-called sum rule), so that

$$N^{(I)(\sigma)} = \sum_{m \in \mathcal{C}^{(I)}} n^{(I)(\sigma)m}_{\quad\ m} = \sum_{m \in \mathcal{C}^{(I)}} n^{(I)(\sigma)m}_{\quad\ m}. \tag{23}$$

Their powers themselves remain tensors, for example the square $n^{2(I)(\sigma)m'}_{\quad\ m} = n^{(I)(\sigma)m''}_{\quad\ m} n^{(I)(\sigma)m'}_{\quad\ m''}$ is itself a well-behaved singly covariant and singly contravariant tensor with an invariant trace. This occupancy matrix trace is easily demonstrated to be invariant under rotations of the set of Hubbard projectors on its site, and it is independent of the basis used to represent the Kohn–Sham states.

An occupancy matrix that is invariant under element-wise transpose might lend itself to an interpretation as quantifying the charge shared between Hubbard projectors, and indeed it does in the case of orthonormal Hubbard projectors. However, it is worth emphasizing that in the case of a set of nonorthogonal Hubbard projectors, these functions are merely spanning vectors with no rigorous physical meaning and, generally, no such interpretation of charge shared between orbitals may be safely made. In fact, in the nonorthogonal case, the occupancy matrix should not be generally expected to be invariant under element-wise transpose, i.e., $n_m^{\ m'} \neq n_m^{Tm'} = n^{m'}_{\ \ m}$. Rather, if the duals are defined in a way which preserves the tensorial consistency of inner products, the occupancy matrix must satisfy instead the more general expression $n_m^{\ m'} = O_{mm''} n^{m''}_{\quad m'''} O^{m'''m'}$, where $O_{\bullet\bullet}$ and $O^{\bullet\bullet}$ are the covariant and contravariant metric tensors, respectively, on the subspace in question. As a result, only the diagonal elements of the occupancy matrix can be imbued with a intuitive meaning in the sense of occupancy; symmetrizing the matrix does not recover such an interpretation for the off-diagonal elements.

III. APPLICATION TO THE DFT+U METHOD

In this section, we illustrate the practical application of the tensorial representation to a particular method for strongly correlated materials, namely, the simplified rotationally invariant DFT+U correction of Refs. 18,21. We provide the necessary expressions for the tensorially invariant DFT+U terms in the energy, potential, and ionic forces for use with nonorthogonal Hubbard projectors, which is of some importance since such a set is often used in contemporary high-accuracy,

particularly linear-scaling, implementations.[8,10–12] We have recently shown that an efficient set of Hubbard projectors can be constructed, which is self-consistent with the set of truncated nonorthogonal generalized Wannier functions which minimize the DFT+U total energy.[15]

In the DFT+U approach, a set $M^{(I)}$ Hubbard projectors, typically spatially localized on a particular transition-metal or lanthanoid atom, is used to define the occupancy matrix of the correlated subspace at each site. The particles occupying these subspaces interact strongly with each other by comparison with their interaction with the bath; each subspace acts as an open quantum system. As such, we may separately impose the Fock antisymmetry condition for the projected wave function for each strongly correlated subspace, so that the subspace occupancy, the projection of the full single-particle density onto the subspace in question, should itself be a valid density matrix operator (it should be idempotent and reproduce the electron number of that subspace).

Since the idempotency of the density matrix for the full system is a condition which must be exactly satisfied, and the idempotency of correlated sites is a competing condition (the Hubbard projectors differ from Kohn–Sham orbitals in general), the subspace idempotency may be only partially enforced, for each correlated site, using an idempotency penalty functional of the form

$$\sum_{I\sigma} \mathrm{Tr}[\hat{\lambda}^{(I)(\sigma)}(\hat{n}^{(I)(\sigma)} - \hat{n}^{(I)(\sigma)2})], \tag{24}$$

which disfavors deviation from wave function antisymmetry in the strongly correlated subspaces. The premultiplier $\hat{\lambda}^{(I)(\sigma)}$ is usually approximated by a single scalar for each site, where it is identified as

$$\hat{\lambda}^{(I)(\sigma)} = \frac{U^{(I)(\sigma)}}{2}, \tag{25}$$

half of the screened, subspace-averaged Coulomb interaction. If we further assume an orthonormal set of Hubbard projectors for each site, the functional is easily recognizable as the familiar rotationally invariant DFT+U correction term of Cococcioni and de Gironcoli in Ref. 18:

$$\sum_{I\sigma} \frac{U^{(I)(\sigma)}}{2}\left[\sum_{m} n_{mm} - \sum_{mm'} n_{mm'}n_{m'm}\right]^{(I)(\sigma)}. \tag{26}$$

A. The tensorially invariant DFT+U functional

Let us consider how we might generalize this DFT+U penalty functional to accommodate an orbital-dependent interaction tensor. The Coulomb interaction tensor U for a given spin channel and site (considering the same Hubbard projectors for different spins for brevity of notation) is given generally by the two-center integral (N.B., using the Dirac, and not Mulliken, convention)

$$U^{(I)}_{mm'm''m'''} = \langle \varphi^{(I)}_{m}\varphi^{(I)}_{m'} | \hat{U}^{(I)(\sigma)}(\mathbf{r},\mathbf{r}') | \varphi^{(I)}_{m''}\varphi^{(I)}_{m'''}\rangle. \tag{27}$$

Here, $\hat{U}^{(\sigma)}(\mathbf{r},\mathbf{r}')$ is the Coulomb interaction screened according to mechanisms described by an appropriate theory such as linear response,[13,18,21] constrained local density approximation (LDA),[22] constrained random-plane approximation (RPA),[23] or constrained adiabatic LDA.[24] Coulomb repulsion is represented by those terms for which $m = m''; m' = m'''$, while direct exchange is given by those elements with $m = m'''$; $m' = m''$.

In the general, nonorthogonal case, care must be taken in employing the U tensor in order to preserve the tensorial invariance of the DFT+U energy. For example, if a tensorial invariant is required which provides the sum of the part of the tensor describing density-density Coulomb repulsions, it should correctly be computed by contracting covariant and contravariant indices in pairs of indices of opposite character, i.e., double-sums of the form (where $m,m' \in \{1,\ldots,M^{(I)}\}$)

$$U_{mm'}{}^{mm'}, \quad U^{mm'}{}_{mm'}, \quad U_{m}{}^{m'm}{}_{m'}, \quad \text{or} \quad U^{m}{}_{m'm}{}^{m'} \tag{28}$$

are admissible while those of the form $U_{mm'mm'}$ or $U^{mm'mm'}$ break tensorial invariance. Indices are raised and lowered simply using the metric tensor of the correlated subspace to which the U tensor corresponds, the contravariant $O^{\bullet\bullet}$ or covariant $O_{\bullet\bullet}$, respectively, e.g.,

$$U_{m}{}^{m'}{}_{m'}{}^{m} = O^{m'm''}U_{mm''m'm'''}O^{m'''m}. \tag{29}$$

Purely as an illustration of this principle, a simple projector-decomposed tensorially invariant penalty functional may be constructed using pairwise contractions over the four indices, as in

$$\sum_{I\sigma} \frac{1}{2}U^{(I)}_{mm''}{}^{m'm'''}\left[n_{m'}{}^{m}\delta_{m'''}{}^{m''} - n_{m'}{}^{m''}n_{m'''}{}^{m}\right]^{(I)(\sigma)}. \tag{30}$$

A commonly used approximation for the screened Coulomb interaction, that which we use, is where the interaction tensor (itself an inverse response function) is averaged over the subspace (i.e., over both perturbing and probing indices), providing a scalar density-density Coulomb interaction. The usual DFT+U penalty functional in this fully averaged approximation is thus given, in tensorially invariant form, by the expression

$$\sum_{I\sigma} \frac{1}{2M^{(I)2}}U^{(I)}_{m''m'''}{}^{m''m'''}\left[n_{m}{}^{m} - n_{m}{}^{m'}n_{m'}{}^{m}\right]^{(I)(\sigma)}. \tag{31}$$

B. DFT+U potential and ionic forces in the tensorial formalism

The DFT+U term in the Kohn–Sham potential, generally given (for real-valued U tensors) by

$$\hat{V}^{(\sigma)} = \sum_{I} |\varphi^{(I)m}\rangle V^{(I)(\sigma)m'}_{m} \langle \varphi^{(I)}_{m'}|, \tag{32}$$

has matrix elements, in the case of averaged U, given by

$$V^{(I)(\sigma)m'}_{m} = \frac{1}{2M^{(I)2}}U^{(I)}_{m''m'''}{}^{m''m'''}\left[\delta_{m}{}^{m'} - 2n^{(I)(\sigma)m'}_{m}\right].$$

The DFT+U potential is Hermitian by construction when the Hubbard projection operator built with the subspace-local tensorial representation of Eq. (19), is used. No symmetrization of the occupancy matrices is then needed to ensure this Hermiticity, and the potential acts strictly within the spatial extent of the subspace on whose occupancy it depends.

Correspondingly, the DFT+U contribution to the force on the ion labeled J, with position $\mathbf{R}_J$, is given by

$$\mathbf{F}_J = -\sum_{I\sigma}\left\langle\frac{d\varphi_m^{(I)}}{d\mathbf{R}_J}\middle|\varphi_{m'}^{(I)}\right\rangle O^{(I)m'm''}n_{m''}^{(I)(\sigma)m'''}V_{m'''}^{(I)(\sigma)m} - \sum_{I\sigma} n_m^{(I)(\sigma)m'}\left\langle\varphi_{m'}^{(I)}\middle|\frac{d\varphi_{m''}^{(I)}}{d\mathbf{R}_J}\right\rangle O^{(I)m''m'''}V_{m'''}^{(I)(\sigma)m}.$$

Here, we have made simplifications such as

$$\left|\frac{d\varphi^{(I)m}}{d\mathbf{R}_J}\right\rangle = \left|\frac{d\varphi_{m'}^{(I)}}{d\mathbf{R}_J}\right\rangle O^{(I)m'm}, \tag{33}$$

which is valid if the subspace metric tensor is position independent, in particular if the Hubbard projectors are simply spatially translated when their host ion is moved. Our force expression holds, of course, only if we are on the Hellmann–Feynman surface, where the density matrix commutes with the Hamiltonian.

IV. BULK NICKEL OXIDE

The first row transition-metal monoxide NiO poses some difficulties to Kohn–Sham DFT and to electronic structure theories generally. As such, it has served as a valuable proving ground for approaches such as periodic unrestricted Hartree–Fock theory,[25] the self-interaction corrected LDA,[2] the GW approximation,[4] and DFT+DMFT.[26] Experimentally, the paramagnetic phase of NiO is found to possess a rock-salt crystal structure with a lattice constant of approximately 4.17 Å.[27] At ambient temperature, NiO is a type-II antiferromagnetic insulator with a local magnetic moment of between $1.64\mu_B$ and $1.9\mu_B$.[18] Due to the persistence of its magnetic moment and optical gap, which is approximately 4 eV, above the Néel temperature, it falls broadly into the category of a Mott insulator[25] with a charge-transfer insulating gap of predominantly oxygen $2p$ to nickel $3d$ orbital character.[25,28] It has long been recognized that LDA-type XC functionals[29] qualitatively fail to reproduce the physics of this material, grossly underestimating the local magnetic moment and the Kohn–Sham gap and assigning an incorrect fully nickel $3d$ orbital character to the valence band edge. We stress, however, that the Kohn–Sham gap is not comparable to the experimental insulating excitation gap, even for the exact XC functional.[30]

The DFT+U method has previously been applied, in numerous incarnations, to bulk NiO, and it is known to recover the principal features of this strongly correlated oxide.[5,13,18,27,31] Moreover, generalizations to DFT+U such as first-principles methods for calculating the Hubbard U parameter,[13,18] the DFT+U+V method for including inter-site interactions,[32] and, most pertinent for this study, previous investigations into subspace representations of nonorthogonal Hubbard projectors in DFT+U,[8,9] have also been applied successfully to this system. We have chosen to study NiO, therefore, because it is so well characterized and we have performed calculations which we hope will be complementary to those described in Ref. 8, where the full, on-site, and dual representations of a linear combination of pseudoatomic orbital basis were compared.

A. Computational methodology

Calculations of the ground-state electronic structure of bulk antiferromagnetic nickel oxide were carried out within collinear spin-polarized Kohn–Sham DFT,[1] and the simplified DFT+U method[18]. The linear-scaling ONETEP first-principles package, described in detail in Refs. 33, was used. The LSDA (PZ81) XC functional,[29] with norm-conserving pseudopotentials,[34,35] was invoked throughout. Periodic boundary conditions were used with a 512-atom supercell and the Brillouin zone was sampled at the Γ point only. A systematic variational basis of Fourier–Lagrange, also known as periodic cardinal sine or *psinc*, functions,[36] was used, equivalent to a set of plane waves bandwidth limited to a kinetic-energy cutoff of 825 eV.

In the ONETEP method, the Kohn–Sham density-matrix is represented in the separable form

$$\rho^{(\sigma)}(\mathbf{r},\mathbf{r}') = \phi_\alpha(\mathbf{r})K^{(\sigma)\alpha\beta}\phi_\beta(\mathbf{r}') \tag{34}$$

in terms of a set of covariant nonorthogonal generalized Wannier functions (NGWFs),[10] $\{\phi_\bullet(\mathbf{r})\}$, and a corresponding contravariant density kernel, $K^{\bullet\bullet}$, for each spin channel. The density kernel was not truncated in the calculations described here. In the ONETEP method,[33] the total energy is iteratively minimized both with respect to the elements of the density kernel for a given set of NGWFs,[37] using a combination of the penalty functional technique[38] and that of Li, Nunes and Vanderbilt (LNV)[39] to ensure the validity of the density matrix, and with respect to the expansion coefficients of the NGWFs in the psinc basis. The converged NGWFs (a minimal set of nine functions for nickel $4s$, $4p$, and $3d$ and four for oxygen $2s$ and $2p$, truncated to an atom-centered sphere of 4.0 Å, were employed in calculations on NiO) are those which are optimized to minimize the total energy and are thus adapted to the chemical environment, incorporating all valence-electron hybridization effects in the ground-state density.

Our principal purpose was to provide an appraisal of the difference in predicted electronic properties, if any, given by DFT+U when using nonorthogonal Hubbard projectors with either the dual or tensorial representations of the correlated subspaces. The dual representation, in particular, was selected for comparison since it appears to be the most sophisticated of the previously proposed subspace definitions – it has a tensorially invariant occupancy matrix trace which cannot be said of the manifestly incomplete on-site and full representations. The latter three representations were previously compared in detail in Ref. 8.

The underestimation of the NiO lattice parameter with respect to experiment by the LDA, as well as the ability of DFT+U to correct this, for a particular U value, has been known for some time.[27] The U parameter required to correct the lattice will depend on details of the underlying XC functional, the precise DFT+U functional used, the pseudopotentials and both the form of the Hubbard projectors and the definition of the subspace projection operators. To provide an unbiased analysis of different subspace definitions, therefore, we employed the same experimental lattice constant for all calculations. To obviate intervention in the construction of the correlated subspaces, so far as possible, we carried out the DFT+U calculations in the projector self-consistent

formalism described in Ref. 15. We also include, for the purposes of comparison, the results of conventional DFT+U calculations using hydrogenic 3d-orbital Hubbard projectors (in which case there is no ambiguity in the representation for a given choice of projectors) which were used as the initial guess for the projector self-consistency cycle.[40]

In the projector self-consistent DFT+U scheme of Ref. 15, the set of five converged NGWFs of maximal 3d-orbital character on a transition-metal atom responsible for strong correlation effects (an example of such as set is illustrated in Fig. 1) is selected as Hubbard projectors to redefine the DFT+U occupancy matrices for the total energy minimization in the next projector iteration. The energy is not directly minimized with respect to the expansion coefficients of the Hubbard projectors (since it would violate the variational principle if either the Hubbard projectors or U were allowed to change during energy minimization[14]), but the projectors are updated in a manner reminiscent of the density-mixing method for solving nonlinear systems,[41] converging toward those which equal a subset of the NGWFs which minimize the DFT+U energy functional which they themselves define. The projector-update process alternates between direct variational minimization of the total energy and projector renewal until both are individually converged.

B. Occupancies and magnetic dipole moments

In agreement with a number of previous studies,[9,27,31] we find that the LDA correctly favors antiferromagnetic ordering in NiO, albeit with diminished local magnetic moments and a greatly underestimated Kohn–Sham gap. The DFT+U correction enhances the antiferromagnetic order with increasing U, monotonically increasing the magnetic dipole moments. Also in accordance with previous work,[8,9] we have found that the DFT+U occupancy matrix and local magnetic dipole moment associated with the correlated subspaces depend significantly on the definition of the correlated subspace projection operator.

Turning first to the total occupancy of the correlated subspaces, shown in Fig. 2, we find a steady decrease with increasing U parameter, which is almost entirely due to the DFT+U correction introducing a repulsive potential to the less-than-half occupied nickel $3d - e_g$ orbitals of the minority spin channel. Conversely, we notice that for the largest element on the diagonal of the occupancy matrix (which is almost identical to that of the other orbitals of the same symmetry), DFT+U introduces an attractive potential that tends to fully occupy the corresponding orbital.

The maximal occupancy element for hydrogenic projectors, for those projectors most commonly used in DFT+U which are not adapted to their chemical environment and so cannot fully account for densities deviating from spherical symmetry, slowly approaches unity, and we conjecture that a rather excessive U value would be needed to complete the orbital filling. On the other hand, if we look at self-consistent NGWF projectors in the dual representation, there is a tendency to overfill the most fully occupied Hubbard projectors, to wit the occupancy begins to exceed unity beyond $U \approx 3$eV. This latter affliction is a rather hazardous one for the DFT+U functional, since the contribution to the energy correction arising from orbitals exhibiting it may become negative in severe cases; this is incorrect behavior for a penalty functional

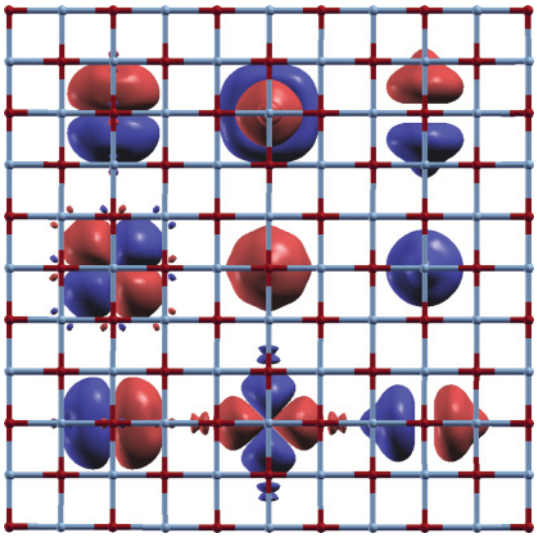

FIG. 1. (Color online) Isosurfaces of the set of nonorthogonal generalized Wannier functions (NGWFs) on a nickel atom in NiO. The NGWFs are those computed at projector self-consistency in the tensorial representation at LDA+U = 6 eV. Those in the left column (predominantly $3d - t_{2g}$ character) and the top and bottom NGWFs in the middle column (predominantly $3d - e_g$ character) are those used as Hubbard projectors, while the remaining NGWFs (pseudized 4s-like in the center and pseudized 4p-like in the right column) lie outside the correlated subspace on that atom. The isosurface is set to half of the maximum for the 4s and 4p-like NGWFs and 10^{-3} times the maximum for the 3d-like NGWFs.

in any case. The reason behind this excessive occupancy is the spurious nonlocality of the Hubbard projector duals in the dual representation; they may pick up density contributions from all across the simulation cell. On the contrary, when self-consistent projectors are used in the tensorial representation, the maximal matrix elements tend asymptotically to unity with increasing U, as expected (reaching 0.9998 at U = 8 eV).

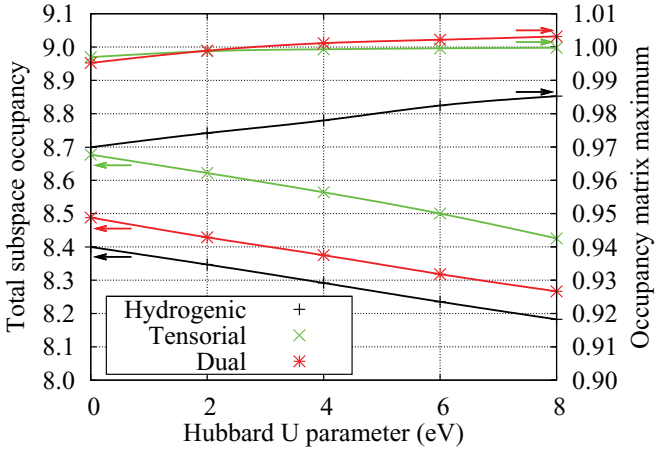

FIG. 2. (Color online) The total occupancy of a correlated subspace in NiO (left axis) and the maximum element on the diagonal of the occupancy matrix (right axis) as functions of the interaction U. Values are computed with orthonormal hydrogenic Hubbard projectors and self-consistent NGWF projectors in both the dual and tensorial representations.

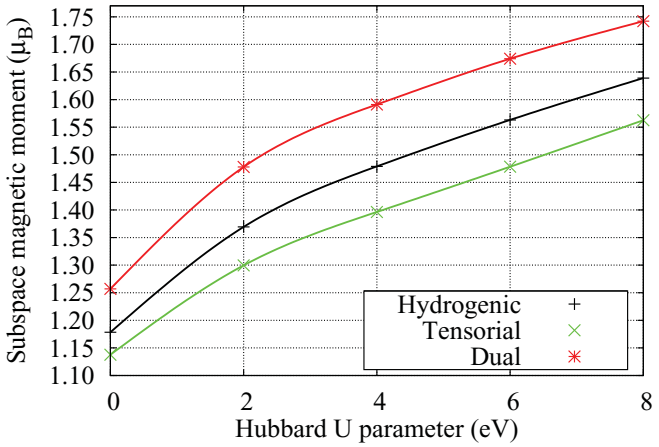

FIG. 3. (Color online) The projection of the magnetic dipole moment onto the DFT+U correlated subspace on nickel atoms in NiO, computed as a function of the interaction U. Values are computed as in Fig. 2.

To test the dependence of our computed DFT properties on the XC functional used for pseudopotential generation, these dependencies known to be potentially substantial when nonlinear core corrections are used,[42] we also performed our "hydrogenic" calculations using LDA[29] pseudopotentials with parameters closely matching to the generalized-gradient approximation (GGA) set.[35] Moving from the latter to the former pseudopotentials, we observed a reduction of the local magnetic moment by $0.007\mu_B$ at $U = 0$ eV, up to $0.02\mu_B$ at $U = 4$ eV, whereat the reduction remains with further increase in U. The total correlated subspace occupancy is rigidly increased by approximately $0.02e$. The maximum occupancy matrix changes by no more than $0.001e$ for any U tested. The occupancy matrices thus depend on the choice of pseudopotential, as expected, as do derived properties, but not sufficiently to influence our observed trends, indeed by a small amount compared with the dependence on the U parameter and subspace projection definition.

Considering the local magnetic moment on the nickel atoms, depicted in Fig. 3 and defined as the difference of the traces of the DFT+U occupancy matrices of the two spin channels, we observe the expected increase with the U parameter as the majority and minority channels of the magnetization-carrying orbitals become increasingly filled or emptied, respectively. The NGWF projectors, in the dual representation yield greater local magnetic moments than the representation-independent hydrogenic projectors and, in turn, those are larger than the moments in the tensorial representation. Consequently, we would expect the exchange splitting which makes up a large contribution to the insulating gap in this material (it is well described within unrestricted Hartree–Fock theory[25]) to follow the same trend. While this behavior may seem a somewhat unfavorable reflection on the tensorial representation, it is fully in line with our understanding that the dual representation (or any related delocalized "Mulliken"-type analysis) picks up additional contributions from magnetization densities of neighboring atoms by construction. The previously demonstrated strong dependence of the moments on the definition of the subspace occupancy matrices,[8] taking the 4 eV spread of U values which approximately yield $1.48\mu_B$ in our calculations as an example, demonstrates the hazard incurred by comparing U parameters used with DFT+U methods that differ in their technical details.

C. Kohn–Sham eigenspectra

The Kohn–Sham eigenspectrum computed for NiO using DFT+U with both our "best-guess" system-independent hydrogenic projectors[40] and self-consistently determined NGWF projectors agree closely. Moreover, in agreement with previous studies of the dependence on the occupancy matrix definition when using nonorthogonal Hubbard projectors,[8,9] the representation dependence of spectral features is rather subtle and is considerably less significant than the dependence on the U parameter. That is not to say, however, that the differences yielded may be guaranteed to be fully recovered by a self-consistent determination or arbitrary variation of the interaction U, since we observe different dependences on this parameter for different spectral peaks, depending on the subspace representation.

Considering, for example, a Hubbard U value within the range of values known to give reasonable agreement with

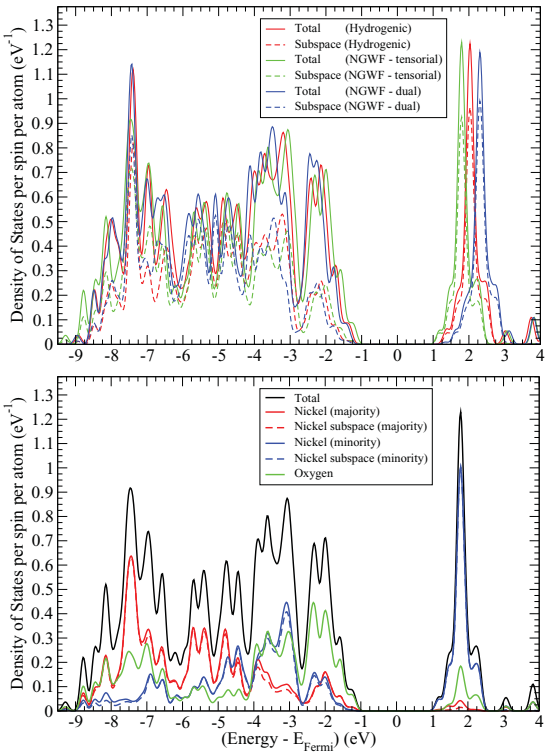

FIG. 4. (Color online) Top: Density of Kohn–Sham states per spin per atom of NiO at LDA+$U = 6$ eV, together with its projection onto the union of correlated subspaces using hydrogenic Hubbard projectors and NGWF projectors in the tensorial and dual representations. Bottom: The decomposition, in the NGWF-tensorial representation, of the density of states for a given spin channel into its contributions from NGWFs on nickel atoms with magnetization aligned (majority) and antialigned (minority) spins, the correlated subspace projections of each, and the contribution due to NGWFs on oxygen atoms.

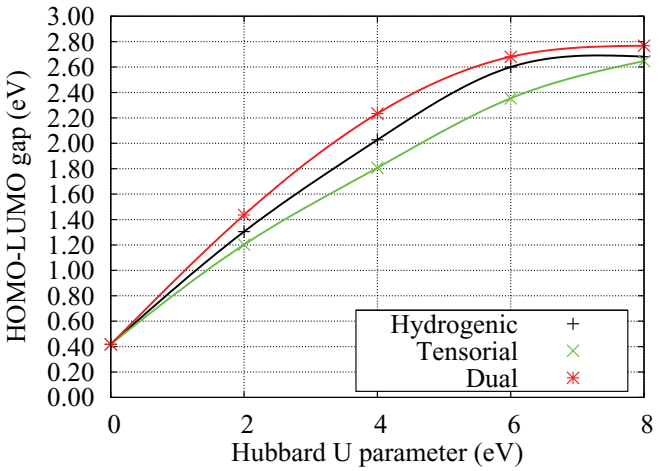

FIG. 5. (Color online) The Hubbard U dependence of the Kohn–Sham band gap of NiO at LDA+U.

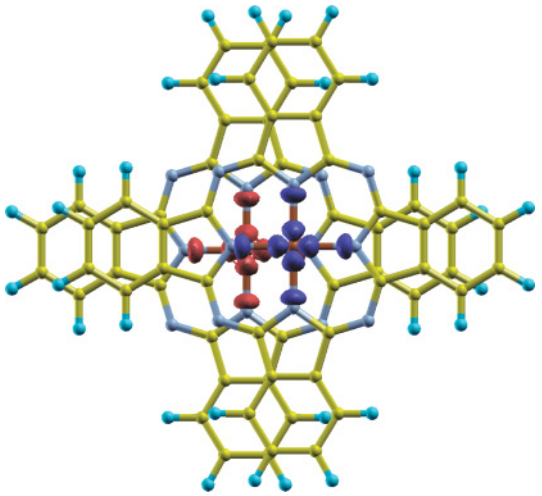

FIG. 6. (Color online) Spin-density isosurfaces at 5% of maximum in Cu(II)Pc_2 at projector self-consistent GGA+U = 6 eV within the NGWF-tensorial subspace representation.

experiment, namely $U = 6$ eV, we have shown the total density of states (DoS), and its correlated subspace projection, in the three representations of interest in the top panel of Fig. 4. The bottom panel shows the decomposition of the tensorial DoS into its contributions from oxygen atoms and both predominantly spin-aligned (majority) or spin-antialigned (minority) nickel atoms. Although all of the dominant features are shared between the eigenspectra of the various representations, there are some discrepancies which are worth noting. Most notable is the trend for the insulating gap to open slightly, predominantly at the minority e_g peak at ≈ 2 eV, as we go from tensorial NGWF (2.35 eV) to hydrogenic (2.60 eV) to dual NGWF representations (2.68 eV). We attribute this to changes in the exchange splitting provided by the enhancement of the magnetic moment, which follows the same trend, as can be seen in Fig. 3. The localized character of the valence band edge is not significantly representation dependent.

We show the U dependence of the Kohn–Sham insulating gap in the three DFT+U correlated subspace definitions in Fig. 5. In all cases, we recover the canonical DFT+U description of this material. With increasing interaction parameter U the tendency is as follows: the low-energy (primarily majority-channel e_g-like) peak falls deeper into the valence band as an attractive potential is applied to fill it completely; the strongly nickel t_{2g}-like valence band edge at the LDA level gives way to hybridized oxygen $2p$ character as the t_{2g}-like states are pushed to lower energies; and the minority-channel nickel e_g-like first peak in the conduction band is increased in energy as its partial occupancy causes it to be subjected to a repulsive corrective potential.

Overall, we reiterate that the effects on the spectra due to the local or nonlocal construction of the Hubbard projector duals, at least in this material, are not sufficiently great to reasonably draw conclusions regarding the relative merit of methods based on agreement, or otherwise, with experimental observations. Rather, in this matter, points of principle such as the preservation of tensorial invariance, or the avoidance of occupancies exceeding unity (as observed in Fig. 2), must therefore take precedence in our view.

V. COPPER PHTHALOCYANINE DIMER

Open-shell molecular systems containing transition-metal ions sometimes pose a challenge to first-principles simulation within LDA-based approximations.[43] This is partially due to the tendency of such approximate XC functionals to excessively delocalize magnetization-carrying orbitals in such systems. As noted in Refs. 21,44–46, both energetic properties, such as magnetic coupling, and also spectroscopic features, such as the nature of the insulating gap and multiplet splittings, can consequently be poorly reproduced by such functionals. Sophisticated *ab initio* techniques such as the GW approximation and local correlation methods such as DFT+U, whose traditional realm of application lies in extended systems such as extended oxides and their interfaces, are being increasingly applied to molecular systems and clusters (see for example Refs. 21,44–47).

It is thus of some importance, and perhaps timely, to consider molecular systems on a similar footing to solids when considering the merit of projection methods for DFT+U. The correlated orbitals in molecular systems may be rather more spatially diffuse and deviate further from spherical symmetry than their counterparts in solids. As a result, the issue of Hubbard projector dependence in DFT+U and then the manner in which the projection operator is constructed from those projectors, particularly the degree of nonlocality in the Hubbard projector duals, can be expected to play a more significant role in the description of molecular systems.

With a view to analyzing the dependence on the correlated subspace definition, or occupancy representation, in the case of molecular systems, we applied our methodology to the ground state of a binuclear open-shell (antiferromagnetically coupled) singlet complex, the copper phthalocyanine dimer denoted α-Cu(II)Pc_2. Crystalline CuPc is a semiconducting blue dye which, in pure thin-film form and more exotic derivatives, is currently attracting intense experimental and theoretical interest due to its potential for use as a flexible organometallic photovoltaic material,[48] as part of field-effect transistors,[49] and, due to its magnetic functionality, in spintronic data

storage or processing devices.[50] In this system, two correlated subspaces delineated by copper $3d$-like states are spatially well separated, with approximately 3.77 Å between centers, and there is minimal electronic bonding between the localized orbitals in the open Cu-$3d$ shells in the two approximately planar moeities. The result is a very weak indirect exchange, i.e., acting via intermediary delocalized ligand states, $S = \frac{1}{2}$ antiferromagnet with a Heisenberg exchange coupling constant of $J \approx -1.50K$; for a detailed analysis of this mechanism see Ref. 51.

It is important to emphasize that although corrective techniques for localized correlation effects such as DFT+U have been shown to be somewhat beneficial in the context of organometallic molecules,[52,53] they are by no means the only, or perhaps favorable, methods for such systems. For Cu(II)Pc_2, as we go on to show, the magnetization carrying copper $3d$ orbitals are partly delocalized and thus not fully recovered by DFT+U. Systems of this type have been described with particular success, notably in Refs. 51,54,55 using hybrid XC functionals comprising a fraction of a nonlocal Hartree–Fock exchange more appropriate to these molecules.

The ONETEP method[33] was used, as before, with Γ-point Brillouin zone sampling, norm-conserving pseudopotentials,[34,35] and a set of nine NGWFs ($4s$, $4p$ and $3d$) for copper ions, four each for carbon and nitrogen ($2s$ and $2p$) and one for hydrogen ($1s$). An NGWF cutoff radius of 5.3 Å and an equivalent kinetic-energy cutoff of 1000 eV were used. The spin-polarized generalized-gradient XC functional of Perdew, Burke and Ernzerof (PBE)[56] was employed. An unsolvated and hydrogenated gas-phase dimer model was extracted[57] from the α(+)Cu(II)Pc_2 polymorph structure, with a stacking angle of 65.1° and a distance between molecular planes of 3.42 Å, giving a lateral offset of 1.58 Å, as reported from transmission electron diffraction analysis described in Ref. 58. A simulation cell of 30 Å × 30 Å × 20 Å provided an interatomic spacing between periodic images of at least 13.5 Å in plane and 16.5 Å out of plane.

A. Magnetic dipole moments

The open-shell singlet fragments of the Cu(II)Pc_2 system consist of single spins, i.e., a moment of $1\mu_B$ on each copper center, aligned antiparallel with respect to each other as illustrated in Fig. 6. Since, however, approximate XC functionals may lower the energy by delocalizing and partially occupying magnetization-carrying orbitals,[43] a diminished value for the local moment is often recovered in practice. The DFT+U method seeks to ameliorate this condition in two complementary ways, that is, by introducing a derivative discontinuity to the energy functional which penalizes fractional occupancies of the spin-orbitals defined by the subspace projections and also, in doing so, by effectively constraining the Kohn–Sham spin-orbitals to more closely resemble the (usually more localized) spatial form of the correlated subspace.

In spite of this, the correlated subspace projected magnetic dipole moments, shown in Fig. 7, indicate that the DFT+U method does not effectively localize the magnetization density to the copper $3d$ manifold for any reasonable value of the U parameter. Using conventional hydrogenic Hubbard

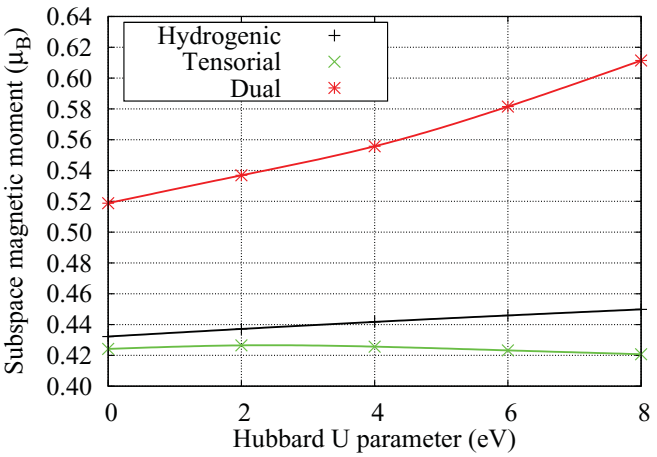

FIG. 7. (Color online) The average magnitude of the projection of the magnetic dipole onto the correlated subspaces of Cu(II)Pc_2, plotted as a function of U for various definitions of the subspace projection.

projectors, with our best guess for the radial profile,[40] we see that there is only a very slight increase in the local moment with U. Switching to self-consistent projectors in the tensorial representation, we find that the moment is effectively U independent and reduced with respect to the hydrogenic result.

Conversely, the dual representation yields a greater magnetic moment than the tensorial representation, by approximately $0.1\mu_B$ at $U = 0$ eV, increasing steadily at a rate of $\approx 0.02\mu_B$ eV^{-1}. The reason for this discrepancy, and failure of DFT+U in this regard, is understood via the atom-decomposed Mulliken analysis of the magnetization density, which gives $0.10 - 0.12\mu_B$ on each nitrogen atom which is a nearest neighbor to copper, irrespective of either the representation or the U parameter. Notwithstanding their adaptation to the molecular environment, the self-consistent NGWF projectors remain predominantly on the copper ion and do not have sufficient weight on the neighboring in-plane nitrogen $2p$ orbitals to capture the magnetization density associated with them. As a result, in the same manner as the conventional projectors, they fail to retrieve the magnetization to the copper $3d_{x^2-y^2}$ orbital within DFT+U. The dual representation, however, partially overcomes this obstacle, due to the dual Hubbard projectors extending over all of the delocalized states in the system, including those that contribute to the magnetization density.

B. Kohn–Sham eigenstates

The accepted understanding[51,54,55] of the spectroscopic nature of the gap in the copper phthalocyanine monomer is that the HOMO level is dominated by a doubly occupied a_{1u} orbital which consists of a superposition of carbon p_z orbitals delocalized on the pyrrole rings of both monomer units, while the spectroscopically correct LUMO level is also a delocalized doubly degenerate orbital, of e_g symmetry composed of a superposition of π orbitals on pairs of macrocycle carbon atoms. We may expect some minor differences in the spectroscopic properties in the dimer system with respect to the monomer,

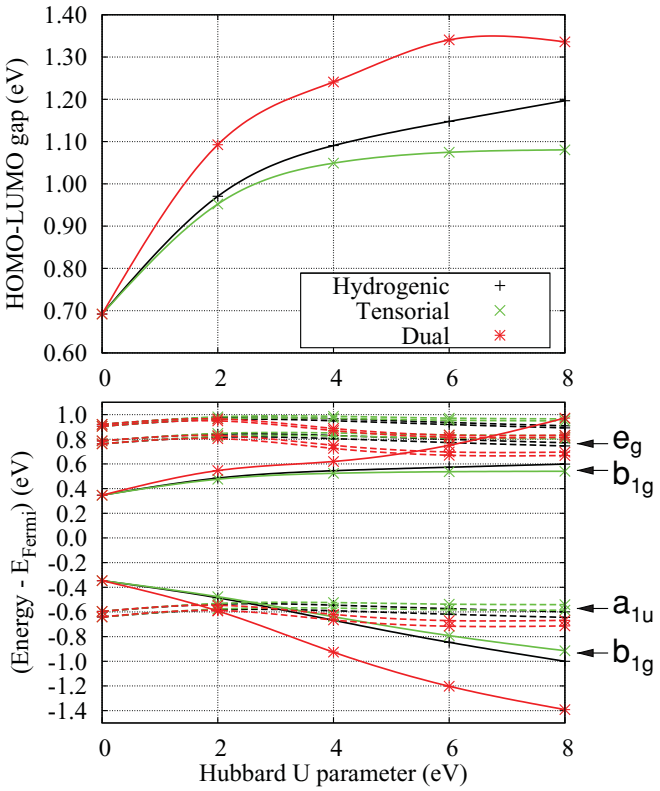

FIG. 8. (Color online) The HOMO-LUMO energy gap (top) and the energy levels adjacent to the Fermi energy (bottom) of Cu(II)Pc_2, plotted as a function of U. In the bottom panel, solid lines show energy levels of states of predominantly Cu-centered b_{1g} character, and to which the DFT+U correction strongly applies, while dashed lines show energy levels of states of more delocalized nature.

due to σ bonding between moieties, but for the main features to be preserved.

It has previously been shown that, due to self-interaction errors, LDA and GGA-type XC functionals do not correctly reproduce the qualitative ordering of states close to the Fermi level in the monomer.[52,54] The DFT+U insulating gap of the dimer system, within various representations, is shown in Fig. 8, along with the U dependence of the states nearest the Fermi energy. For the spin-polarized PBE functional, we find a gap of 0.7 eV for the dimer, whose nature is a charge-transfer excitation between b_{1g} orbitals on either moiety. The b_{1g} orbital is that which carries the magnetization density in the dimer, consisting primarily of copper $3d_{x^2-y^2}$ σ-bonded to in-plane nitrogen $2p$. The representation dependence of the HOMO-LUMO (highest occupied molecular orbital to lowest unoccupied molecular orbital) gap follows the same trend as the local magnetic moment, due to the DFT+U correction to the Coulomb-repulsion gap being somewhat augmented by an associated enhancement to the exchange splitting. In the case of the HOMO orbital, a small value of U is needed to push the singly-occupied b_{1g} state to its spectroscopically correct position below the a_{1u} state, and the effect is rather more strongly pronounced in the dual representation than in the spatially localized methods.

The incomparability between Kohn–Sham eigenenergies with either experimental optical or photoemission spectra notwithstanding, it is perhaps worth noting some similarities and differences between our computed Kohn–Sham levels for the dimer system and the gas-phase ultraviolet photoelectron spectra (UPS) and x-ray absorption near edge structure (XANES) reported in Ref. 55. Turning first to the valence band edge, the UPS confirm that single-molecule CuPc possesses a doubly occupied HOMO of pyrrole-delocalized a_{1u} character, while a further weak ionization peak at 800 meV above that is consistent with the magnetization-carrying copper $3d_{x^2-y^2}$-based b_{1g} orbital seen, albeit substantially closer to the valence band edge for moderate U values, in Fig. 8. This may suggest a suppression of spin splitting between the b_{1g} levels in the dimer over the monomer system, or may be due to an underestimation of experimental transition energies which is not sufficiently alleviated by DFT+U. In the case of the lowest conduction bands, carbon K edge XANES spectra assign a large pyrrole carbon character to the LUMO, consistent with a delocalized and degenerate e_g type orbital. Due to the differing localization regions of the carbon $1s$ and singly occupied b_{1g} orbital, as noted in Ref. 55, such excitations are neglected and so we cannot compare our prediction that the latter orbital lies somewhat below the e_g level for all except the dual representation at high U values. We agree on the proximity of these latter levels with previous monomer calculations using the PBE functional.[53,54]

The tensorial and hydrogenic representations have similar effects, as expected; the effect of projector self consistency is rather small in this system. In the case of the virtual orbitals, the localized b_{1g} character of the LUMO persists for the tensorial and hydrogenic methods, which agree quite closely, while $U \geqslant 6$ eV is sufficient to expose a delocalized e_g orbital as LUMO in the dual representation. There is necessarily some small perturbative effect on delocalized orbitals induced by changes to those which are DFT+U corrected, which is evident in all projection techniques but noticeably stronger in the dual representation.

The overall result is that, for this hybridized correlated system, the dual representation recovers the expected magnetic dipole moment with significantly more success than the fully localized projections. The spectroscopic nature of the insulating gap is also recovered to a greater degree for a given value of U. We would contend, however, that it does so for reasons not expected in the DFT+U method. Specifically, where the local magnetic moment as measured by the dual projectors increases with increasing U, the spatial distribution of this increase is made up both of the region immediately surrounding the copper ion and spatially diffuse contributions, as opposed to the tensorial or conventional orthonormal hydrogenic contributions, with which we are guaranteed to include only subspace-localized densities.

VI. CONCLUDING REMARKS

We have presented a revised formalism for the construction of projection operators, and consequently the occupancy matrices, of strongly correlated subspaces using nonorthogonal Hubbard projector functions in *ab initio* methods such as DFT+U and DFT+DMFT. In contrast to the previously proposed full[13], on-site,[14] and dual[8] representations, our tensorial definition preserves the important property of tensorial

invariance in the total occupancy of each subspace, the total energy, and the ionic forces, by construction. The required expressions for the tensorially invariant DFT+U energy functional and the resulting potential and ionic forces have been presented.

Localized nonorthogonal basis functions for Kohn–Sham states are frequently used to represent the Hubbard projectors, in practice, either for reasons of computational convenience or to achieve projector self-consistency.[15] We have shown, however, that it is inappropriate to continue to identify the dual space (and the metric tensor) of the basis functions with the dual space of Hubbard projectors on each site. For molecular systems, in particular, the unexpected discrepancy with respect to orthonormal projectors that is thereby introduced may be significant. The resulting projector duals (contravariant vectors) are unsuited to constructing a correction for localized correlation effects, generally being delocalized across the entire simulation cell. When using delocalized projector duals, moreover, a tensor-incompatible symmetrization of the projection operator is needed to ensure a Hermitian potential. This may result in unphysical occupancy matrix elements and an uncontrolled action of the corrective potential which it defines. Put simply, additional nonlocal corrections are introduced in the dual representation which are extraneous to the requirement of accounting for the nonorthogonality of the Hubbard projectors.

Our tensorial formalism may be implemented in any methodology which makes use of a nonorthogonal set of functions to define each correlated subspace. Since it inherently preserves the spatial localization of Hubbard projector duals, it is also less computationally expensive and simpler to implement in linear-scaling methods, in practice, than the on-site or dual representations which employ delocalized dual projectors. To alleviate the remaining arbitrariness in DFT+U and related methods in the nonorthogonal case, the tensorial formalism may be combined with both a projector self-consistency algorithm[15] or any one of a number of available first-principles methods for the U parameter,[13,18,21–24] the latter remains as an avenue for future investigation.

It is our hope that we have dispelled some of the ambiguities surrounding this topic which we feel have arisen inevitably as a result of the neglect of the invaluable tensor notation. As the use of linear-scaling *ab initio* approaches becomes increasingly widespread, we envisage that this work may aid the routine implementation of sophisticated functionality in the nonorthogonal bases, obviating the expenditure of explicit orthonormalization.

ACKNOWLEDGMENTS

We would like to thank Nicholas Hine for helpful discussions. This research was supported by EPSRC, RCUK, and the National University of Ireland. Calculations were performed on the Cambridge HPCS Darwin computer under EPSRC Grant No. EP/F032773/1 and the UK National Supercomputing Service HECToR computer with support from the UKCP consortium.

APPENDIX A: ORTHONORMAL HUBBARD PROJECTORS

Orthonormal sets of Hubbard projectors, as well as nonorthogonal sets, may provide a compact and accurate representation of the correlated subspaces and we would not wish to detract from their value and ease of use. In the orthonormal case, the Hubbard projectors equal their own duals with respect to their subspace, and the metric tensors reduce to Kronecker delta functions.

If one performs an inverse Löwdin transform[16] from an orthonormal set of projectors to a nonorthogonal frame using the matrix square root of covariant and contravariant metrics on a particular correlated subspace, $O^{\frac{1}{2}}$ and $O^{-\frac{1}{2}}$, respectively, then the premultiplicative scalar U parameter for that site remains identically the same, since for each site (if n and n' index orthonormal projectors and m and m' index their nonorthogonal counterparts) we have, supposing $n,n',m,m' \in \{1,\ldots,M^{(I)}\}$,

$$\begin{aligned}\sum_{nn'} U_{nn'nn'} &= \sum_{nn'n''n'''} U_{nn'n''n'''}\delta_{nn''}\delta_{n'n'''} \\ &= \sum_{nn'}\sum_{n''n'''} U_{nn'n''n'''}\sum_{mm'} O^{\frac{1}{2}}_{nm} O^{-\frac{1}{2}mn''} O^{\frac{1}{2}}_{n'm'} O^{-\frac{1}{2}m'n'''} \\ &= \sum_{mm'} U_{mm'}{}^{mm'} \equiv M^{(I)2}U.\end{aligned}$$

Thus, when the Coulomb interaction is approximated by a premultiplicative scalar U times the identity, we retain its usual interpretation as the averaged screened Coulomb repulsion between densities in the subspace described by the Hubbard projectors, regardless of whether or not the Hubbard projectors are orthonormal.

APPENDIX B: INVARIANCE UNDER GENERALIZED LÖWDIN TRANSFORMS

As suggested in Ref. 9, generalized definitions of the Löwdin transform may be envisaged whereby the metric tensor is raised to an arbitrary power A, as is its inverse, and the canonical Löwdin transform $A = \frac{1}{2}$ has the status of a special case. Since, however, by construction

$$\delta_n{}^{n'} = \sum_{m\in\mathcal{C}^{(I)}} O^{(I)(A)}_{nm} O^{(I)(-A)mn'} = \sum_{\gamma\in\mathcal{S}} S^{(A)}_{n\gamma} S^{(-A)\gamma n'},$$

the fully averaged scalar U is invariant under such transformations, independent of the exponent A, regardless of whether the subspace metric tensor $O_{\bullet\bullet}$ or, in the dual representation case, the metric $S_{\bullet\bullet}$ on the space spanned by all basis functions, $\mathcal{S}$, is used.

In the latter case of $S_{\bullet\bullet}$, the generalized Löwdin transformation exponent A varies the nonorthogonality of the representation of the occupancy matrices or, equivalently, (since the basis set metric S introduces spurious contributions to the occupancy matrix from across the simulation cell) the degree of nonlocality of the correction. The dependence of computed ground-state properties and of the Kohn–Sham gap of a variety of materials on A, as reported in Ref. 9, demonstrates, in our view, the ambiguity of population analysis measures, and hence corrections such as DFT+U, which are built from tensorially inconsistent (necessarily

symmetrized) occupancy matrices where delocalized Hubbard projector duals of the form $|\varphi^{(I)m}\rangle = \sum_{\gamma\in\mathcal{S}} |\varphi^{(I)}_{\gamma}\rangle S^{(-A)\gamma m}$ are used in the construction of the Hubbard projectors.

The observation of Ref. 9 that the A parameter bears influence on computed properties accords well with our arguments on the unsuitability of the metric $S^{\bullet\bullet}$ (that for the basis functions in the entire simulation cell) in constructing localized self-interaction corrections such as DFT+U, since that parameter effectively controls the superfluous spatial delocalization of the Hubbard projector duals and hence the severity of the tensorial inconsistency in the DFT+U functional. By varying A, the occupancy matrix for the dual representation subject to a generalized Löwdin transformation, given by

$$\sum_{\gamma,\delta\in\mathcal{S}} S^{(A)m\gamma}\langle\varphi^{(I)}_{\gamma}|\hat{\rho}|\varphi^{(I)}_{\delta}\rangle S^{(1-A)\delta m'},$$

picks up differing nonlocal contributions (densities from outside the correlated subspace). Spurious nonlocal contributions are incorporated for all values of A, moreover.

On the contrary, in the tensorial representation, the generalized Löwdin transformed occupancy matrix,

$$\sum_{m'',m'''\in\mathcal{C}^{(I)}} O^{(I)(A)mm''}\langle\varphi^{(I)}_{m''}|\hat{\rho}|\varphi^{(I)}_{m'''}\rangle O^{(I)(1-A)m'''m'},$$

contains no contributions from outside the correlated subspace it is describing for any value of A. Both the trace of this matrix and the trace of its square are entirely independent of A, since $O^{(I)(1-A)m'''m}O^{(I)(A)mm''} = O^{(I)m'''m''}$. Thus, by construction, the DFT+U correction is invariant under generalized Löwdin transformations and so is unambiguously defined, for a given choice of projectors, when the appropriate subspace-local metric tensor $O^{\bullet\bullet}$ is used to build the projection operator.

*ddo20@cam.ac.uk

[1] P. Hohenberg and W. Kohn, Phys. Rev. **136**, B864 (1964); W. Kohn and L. J. Sham, *ibid.* **140**, A1133 (1965).

[2] A. Svane and O. Gunnarsson, Phys. Rev. Lett. **65**, 1148 (1990).

[3] E. Engel and R. N. Schmid, Phys. Rev. Lett. **103**, 036404 (2009).

[4] F. Aryasetiawan and O. Gunnarsson, Phys. Rev. Lett. **74**, 3221 (1995).

[5] V. I. Anisimov, J. Zaanen, and O. K. Andersen, Phys. Rev. B **44**, 943 (1991); V. I. Anisimov, I. V. Solovyev, M. A. Korotin, M. T. Czyżyk, and G. A. Sawatzky, *ibid.* **48**, 16929 (1993).

[6] V. I. Anisimov, A. I. Poteryaev, M. A. Korotin, A. O. Anokhin, and G. Kotliar, J. Phys. Condens. Matter **9**, 7359 (1997); A. I. Lichtenstein and M. I. Katsnelson, Phys. Rev. B **57**, 6884 (1998).

[7] J. Hubbard, Proc. R. Soc. London A **276**, 238 (1963); **277**, 237 (1964); **281**, 401 (1964).

[8] M. J. Han, T. Ozaki, and J. Yu, Phys. Rev. B **73**, 045110 (2006).

[9] C. Tablero, J. Phys. Condens. Matter **20**, 325205 (2008).

[10] C.-K. Skylaris, A. A. Mostofi, P. D. Haynes, O. Diéguez, and M. C. Payne, Phys. Rev. B **66**, 035119 (2002).

[11] E. Hernández and M. J. Gillan, Phys. Rev. B **51**, 10157 (1995).

[12] F. Mauri and G. Galli, Phys. Rev. B **50**, 4316 (1994).

[13] W. E. Pickett, S. C. Erwin, and E. C. Ethridge, Phys. Rev. B **58**, 1201 (1998).

[14] K. K. H. Eschrig and I. Chaplygin, J. Solid State Chem. **176**, 482 (2003).

[15] D. D. O'Regan, N. D. M. Hine, M. C. Payne, and A. A. Mostofi, Phys. Rev. B **82**, 081102 (2010).

[16] P. O. Löwdin, J. Chem. Phys. **18**, 365 (1950).

[17] E. Artacho and L. Miláns del Bosch, Phys. Rev. A **43**, 5770 (1991); C. A. White, P. Maslen, M. S. Lee, and M. Head-Gordon, Chem. Phys. Lett. **276**, 133 (1997).

[18] M. Cococcioni and S. de Gironcoli, Phys. Rev. B **71**, 035105 (2005).

[19] R. S. Mulliken, J. Chem. Phys. **23**, 1833 (1955).

[20] A. Einstein, Ann. Phys. **354**, 769 (1916).

[21] H. J. Kulik, M. Cococcioni, D. A. Scherlis, and N. Marzari, Phys. Rev. Lett. **97**, 103001 (2006).

[22] O. Gunnarsson, O. K. Andersen, O. Jepsen, and J. Zaanen, Phys. Rev. B **39**, 1708 (1989); V. I. Anisimov and O. Gunnarsson, *ibid.* **43**, 7570 (1991); K. Nakamura, R. Arita, Y. Yoshimoto, and S. Tsuneyuki, *ibid.* **74**, 235113 (2006).

[23] F. Aryasetiawan, M. Imada, A. Georges, G. Kotliar, S. Biermann, and A. I. Lichtenstein, Phys. Rev. B **70**, 195104 (2004); K. Karlsson, F. Aryasetiawan, and O. Jepsen, *ibid.* **81**, 245113 (2010).

[24] F. Aryasetiawan, K. Karlsson, O. Jepsen, and U. Schönberger, Phys. Rev. B **74**, 125106 (2006).

[25] M. D. Towler, N. L. Allan, N. M. Harrison, V. R. Saunders, W. C. Mackrodt, and E. Aprà, Phys. Rev. B **50**, 5041 (1994).

[26] X. Ren, I. Leonov, G. Keller, M. Kollar, I. Nekrasov, and D. Vollhardt, Phys. Rev. B **74**, 195114 (2006).

[27] S. L. Dudarev, G. A. Botton, S. Y. Savrasov, C. J. Humphreys, and A. P. Sutton, Phys. Rev. B **57**, 1505 (1998).

[28] G. A. Sawatzky and J. W. Allen, Phys. Rev. Lett. **53**, 2339 (1984).

[29] J. P. Perdew and A. Zunger, Phys. Rev. B **23**, 5048 (1981).

[30] J. P. Perdew and M. Levy, Phys. Rev. Lett. **51**, 1884 (1983).

[31] O. Bengone, M. Alouani, P. Blöchl, and J. Hugel, Phys. Rev. B **62**, 16392 (2000).

[32] V. L. Campo Jr and M. Cococcioni, J. Phys. Condens. Matter **22**, 055602 (2010).

[33] C.-K. Skylaris, P. D. Haynes, A. A. Mostofi, and M. C. Payne, J. Chem. Phys. **122**, 084119 (2005); P. D. Haynes, C.-K. Skylaris, A. A. Mostofi, and M. C. Payne, Chem. Phys. Lett. **422**, 345 (2006).

[34] A. M. Rappe, K. M. Rabe, E. Kaxiras, and J. D. Joannopoulos, Phys. Rev. B **41**, 1227 (1990).

[35] A set of RRKJ Pseudopotentials were generated using the Opium code, [http://opium.sourceforge.net], using the GGA input parameters available therein, optimized for a minimum plane-wave cutoff of 680 eV, albeit with a scalar-relativistic correction for all species and, for the transition-metal ions, some slight modifications to the core radii and a nonlinear core correction of cutoff radius 1.3 a.u.

[36] A. A. Mostofi, P. D. Haynes, C.-K. Skylaris, and M. C. Payne, J. Chem. Phys. **119**, 8842 (2003); D. Baye and P.-H. Heenen, J. Phys. A **19**, 2041 (1986).

[37]P. D. Haynes, C.-K. Skylaris, A. A. Mostofi, and M. C. Payne, J. Phys. Condens. Matter **20**, 294207 (2008).
[38]R. McWeeny, Rev. Mod. Phys. **32**, 335 (1960).
[39]X.-P. Li, R. W. Nunes, and D. Vanderbilt, Phys. Rev. B **47**, 10891 (1993); R. W. Nunes and D. Vanderbilt, *ibid*. **50**, 17611 (1994); M. S. Daw, *ibid*. **47**, 10895 (1993).
[40]The effective nuclear charge Z used to construct the hydrogenic projectors, which may influence predicted observables in the case of system-independent Hubbard projectors[13,15] but which does not significantly influence results at projector self-consistency, was estimated by fitting the hydrogenic radial probability density to that of the corresponding valence pseudo-orbitals in the sense of least-squared deviations (resulting in $Z = 9.02$ and $Z = 9.10$ for $3d$-orbital projectors in nickel and copper, respectively).
[41]D. G. Anderson, J. ACM **12**, 547 (1965); C. G. Broyden, Math. Comput. **19**, 577 (1965).
[42]M. Fuchs, M. Bockstedte, E. Pehlke, and M. Scheffler, Phys. Rev. B **57**, 2134 (1998).
[43]A. J. Cohen, P. Mori-Sanchez, and W. Yang, Science **321**, 792 (2008).
[44]K. Palotás, A. N. Andriotis, and A. Lappas, Phys. Rev. B **81**, 075403 (2010).
[45]D. W. Boukhvalov, A. I. Lichtenstein, V. V. Dobrovitski, M. I. Katsnelson, B. N. Harmon, V. V. Mazurenko, and V. I. Anisimov, Phys. Rev. B **65**, 184435 (2002).
[46]D. A. Scherlis, M. Cococcioni, P. Sit, and N. Marzari, J. Phys. Chem. B **111**, 7384 (2007).
[47]L. G. G. V. Dias da Silva, M. L. Tiago, S. E. Ulloa, F. A. Reboredo, and E. Dagotto, Phys. Rev. B **80**, 155443 (2009).
[48]Z. Bao, A. J. Lovinger, and A. Dodabalapur, Appl. Phys. Lett. **69**, 3066 (1996).
[49]P. Peumans, S. Uchida, and S. R. Forrest, Nature (London) **425**, 158 (2003).
[50]M. Cinchetti, K. Heimer, J.-P. Wüstenberg, O. Andreyev, M. Bauer, S. Lach, C. Ziegler, Y. Gao, and M. Aeschlimann, Nat. Mater. **8**, 115 (2009).
[51]W. Wu, A. Kerridge, A. H. Harker, and A. J. Fisher, Phys. Rev. B **77**, 184403 (2008).
[52]H. Vázquez, P. Jelínek, M. Brandbyge, A. Jauho, and F. Flores, Appl. Phys. A **95**, 257 (2009).
[53]A. Calzolari, A. Ferretti, and M. B. Nardelli, Nanotechnology **18**, 424013 (2007).
[54]N. Marom, O. Hod, G. E. Scuseria, and L. Kronik, J. Chem. Phys. **128**, 164107 (2008).
[55]F. Evangelista, V. Carravetta, G. Stefani, B. Jansik, M. Alagia, S. Stranges, and A. Ruocco, J. Chem. Phys. **126**, 124709 (2007).
[56]J. P. Perdew, K. Burke, and M. Ernzerhof, Phys. Rev. Lett. **77**, 3865 (1996).
[57]We acknowledge and thank Nina Kearsey for her kind provision of the extracted dimer structure.
[58]A. Hoshino, Y. Takenaka, and H. Miyaji, Acta Crystallogr. Sec. B **59**, 393 (2003).